Thermal Variability of the Tropical Tropopause Region Derived From GPS/MET Observations

William J. Randel and Fei Wu
NCAR
Boulder, CO

Waleska Rivera Ríos
University of Texas at El Paso
El Paso, TX

Revised September 2002

Abstract

Structure and variability of temperatures in the tropical upper troposphere and lower stratosphere (~10-30 km) are studied based on Global Positioning System Meteorology (GPS/MET) observations during April 1995-February 1997. Comparisons with several hundred co-located radiosondes demonstrates the high accuracy of GPS/MET retrievals in the tropics. Mean structure and variability of the tropical cold point tropopause is examined, and much of the sub-seasonal variability in cold point temperature and height appears to be related to wave-like fluctuations (such as gravity waves or Kelvin waves). Significant correlations are found between the GPS/MET temperatures and daily, gridded outgoing longwave radiation data (a proxy for tropical deep convection), providing independent confirmation of the GPS/MET temperature fluctuations. These correlations quantify the large-scale tropical temperature response to transient convection, showing coherent wave-like variations over ~12-18 km which span a hemisphere in longitude. The GPS/MET data also show clear evidence of the stratospheric quasi-biennial oscillation (QBO) in temperatures over altitudes ~16-40 km.

1. Introduction

The meteorological behavior of the tropical tropopause region is of interest for quantifying climate variability and change, and for understanding mechanisms of troposphere-stratosphere coupling. The climatological structure and variability of the tropical tropopause, and mechanisms which maintain that structure, are topics of active research [e.g., *Highwood and Hoskins*, 1998; *Thuburn and Craig*, 2000, 2002; *Kiladis et al.*, 2000; *Seidel et al.,* 2001; *Gettelman and Forster*, 2002; *Folkins*, 2002]. Further more, current interests in stratospheric dehydration and water vapor trends (SPARC, 2001), and the formation mechanisms of tropical thin cirrus clouds [*Jensen et al.,* 1996; *Massie et al.,* 2002] both require accurate estimates of temperature and circulation near the tropical tropopause. Observational data in this region are based primarily on the global radiosonde network, with large data sparse regions [e.g., *Highwood and Hoskins*, 1998; *Seidel et al.,* 2001], or operational meteorological analyses, with relatively low vertical resolution and attendant biases [e.g., *Hoinka*, 1998; *Randel et al.,* 2000].

In this work we use a relatively new temperature profile data set, derived from Global Positioning System Meteorology (GPS/MET) radio occultation measurements [*Kursinski et al.,* 1996; *Rocken et al.,* 1997], to analyze the structure and variability of temperatures in the upper troposphere and lower stratosphere (UTLS) during April 1995-February 1997. These GPS/MET data have the advantage of high vertical resolution, plus relatively dense spatial sampling for selected time periods. *Nishida et al.* [2000] have used these data to examine aspects of the mean tropopause structure, including its seasonal and longitudinal variation. Our work extends their analyses in that we focus on variability evident in the GPS/MET data, in particular for sub-seasonal variability of the cold point tropopause. Although the seasonal changes in tropical tropopause structure are

reasonably well understood from empirical analyses [e.g., *Seidel et al.,* 2001], relatively less is known about transient behavior or the mechanisms which influence the cold point temperature and height. In order to quantify the influence of deep convection on temperatures in the tropical tropopause region, our analyses examine statistical relationships between the GPS/MET temperature data and daily, gridded outgoing longwave radiation (OLR) measurements. The results show coherent large-scale temperature responses to transient convection in the tropical tropopause region, including variability near the cold point. We also use the long record and high vertical resolution of GPS/MET data to quantify seasonal and interannual changes in tropical temperatures over the region ~10-40 km, and in particular isolate the detailed signatures of the annual cycle and the stratospheric quasi-biennial oscillation (QBO).

2. Data and Analyses

a. GPS/MET temperature data

The GPS/MET Program was established in 1993 by the University Corporation for Atmospheric Research (UCAR) to demonstrate active limb sounding of the Earth's atmosphere using the radio occultation technique [*Rocken et al.,* 1997]. This demonstration system measured occulted GPS satellite signals from a low orbiting satellite (MicroLab-1), with occultations occurring as the instrument sets below the Earth's horizon relative to any of the constellation of 24 GPS satellites. The arrival time of the GPS signal at the instrument is delayed because of refractive bending in the atmosphere, and this information can be used to derive an altitude profile of the atmospheric refractive index. In the neutral atmosphere (below ~100 km) the refractive index is primarily a function of temperature and relative humidity; above approximately 10 km the atmosphere is effectively dry, so that the GPS/MET measurements can be used

to derive the profile of temperature. Because of inversion details, data above ~40-50 km are highly influenced by climatology, and hence the GPS/MET temperature data analyzed here are most useful for the region ~10-40 km. The horizontal scale associated with the GPS/MET temperature retrievals is ~300 km (this is the horizontal distance which contributes information along the occultation ray path), and the vertical resolution in the upper troposphere-lower stratosphere (UTLS) is of order 1 km (the data are gridded on a 0.2 km vertical grid). The local time of the measurements varies randomly throughout the day. Further details of GPS/MET and derived temperatures can be found in *Rocken et al.* [1997] and *Kursinski et al.* [1997].

GPS/MET provided occultation measurements for the period April 1995-February 1997. The number of retrieved temperature profiles (and their quality) varies over time with between 0 to ~2000 profiles for individual months [as listed in Table 1 of *Nishida et al.,* 2000]. Along with examining overall seasonal and interannual temperature changes in these data, we focus on details of tropopause variability for two periods with most dense sampling, June-July 1995 and December-February (DJF), 1996-1997. The June-July 1995 and February 1997 time periods also have the highest data quality, so-called 'prime times' associated with encryption of the GPS signal [*Rocken et al.,* 1997].

b. OLR data

In order to study coherence with tropical convection, we include here analyses of outgoing long wave radiation (OLR) data as a proxy for tropical convection. Daily gridded OLR data are obtained from the Climate Diagnostics Center web site http://www.cdc.noaa.gov. These daily data are available on a 2.5 degree latitude-longitude grid, with data gaps filled by interpolation to provide complete sampling.

3. Comparisons With Radiosondes and Global Analyses

Rocken et al. [1997] have made extensive comparisons between GPS/MET temperature profiles and a number of correlative data sets (radiosondes, meteorological analyses and satellite data), with main focus on the global atmosphere. Because of the tropical focus of this paper, we have made further comparisons between GPS/MET and nearby radiosonde temperature profiles only in the tropics (20°N-S). These comparisons span the 1995-1997 time period, and the statistics are calculated separately for the GPS/MET prime times (June-July 1995 and February 1997) and off-prime times (all other months), in order to test for any systematic differences. We use co-location criteria between the GPS/MET and radiosonde data of ± 12 hours and 3 degrees great circle distance (approximately 330 km, consistent with the 300 km horizontal scale of GPS/MET). Mean and rms temperature differences are shown in Figure 2 for profiles over 10-30 km, based on ~50-150 comparisons for each time period (decreasing with altitude, due to radiosonde balloon bursts). The mean temperature differences are within ~ ± 1°K over this altitude region, with small positive differences just above the tropopause (~ 17-20), for both time periods. However, the GPS/MET – radiosonde rms differences are of order 2-3 K over 10-30 km, so that none of the mean biases are statistically significant. Note this ~2-3 K rms difference is approximately the same size as radiosonde temperature variances in the UTLS [e.g., *Tsuda et al.,* 1994], so that the results in Figure 2 are consistent with this level of 'natural' variability. Larger biases are seen in Figure 2 at and below 10 km, due to growing influence of water vapor on the GPS/MET retrievals. The rms differences are just slightly larger (~10-20%) for the off-prime GPS/MET measurements, but overall the statistics are similar for both time samples, suggesting the prime and off-prime GPS/MET measurements have similar

quality. Direct comparison of the cold point tropopause (temperature minimum) between these data sets gives mean and rms (GPS/MET – radiosonde) differences of 0.6 ± 2.7 K for temperature, and –0.1 ± 0.9 km for altitude (not dependent on time period). These statistical comparisons over the entire tropics are consistent with the results over Indonesia discussed by *Nishida et al.,* 2000. Overall these comparisons suggest that the GPS/MET temperatures are of high quality in the tropics over ~10-30 km and not strongly dependent on the GPS signal encryption, so that their high spatial sampling can significantly augment the tropical radiosonde network.

A further comparison of temperature profiles in the tropics (10°N-S) is shown in Figure 3, showing the January 1-15, 1997 time mean profile derived from GPS/MET with results from several operational meteorological analyses: NCEP/NCAR reanalyses [*Kalnay et al.,* 1996], ECMWF analyses, and UKMO stratosphere-troposphere assimilation [*Swinbank and O'Neill*, 1994]. Note that the vertical resolution of these analyzed data sets in the UTLS is ~2.5-3.0 km. These comparisons show significant differences near the tropopause (~17 km), where the analyses do not capture the depth or sharpness of the cold point, due primarily to the lack of vertical resolution [as discussed previously in *Pawson and Fiorino*, 1998, and *Randel et al.,* 2000]. A further region of difference is seen above ~24 km, where the GPS/MET temperatures are higher than temperatures in the analyses. This temperature 'bulge' in the GPS/MET data in January 1997 is associated with the QBO, as shown below in Figure 16. A weaker amplitude QBO 'bulge' is also seen in the UKMO data in Figure 3, but the QBO is less evident in the NCEP/NCAR and ECMWF data.

4. Structure and Variability of the Tropical Tropopause Region

a. Time mean structure

The space-time sampling of GPS/MET is most suitable for studying the spatial structure of the tropopause for seasonal means. Here the spatial structure is estimated using a simple Gaussian weighted binning analysis (on a 4° latitude by 30° longitude grid, using Gaussian half-widths of 5° latitude and 50° longitude). Figure 4 shows the individual cold point temperature and height measurements over 10°N-S during DJF 1996-1997, together with the binned seasonal mean values. Note the considerable amount of variability about the time mean that is observed within a season, which is explored in more detail below.

The spatial structures of cold point tropopause temperature (T_{CP}) and altitude (Z_{CP}) derived from GPS/MET for JJ 1995 and DJF 1996-1997 is shown in Figure 5. The spatial patterns for these individual seasons are consistent with previous radiosonde-based climatologies [e.g., *Highwood and Hoskins*, 1998; *Seidel et al.,* 2001] and with meteorological analyses [e.g., *Hoinka*, 1998; *Randel et al.,* 2000]. The coldest tropopause temperatures during DJF are ~188 K, located over a wide region in the tropical western Pacific, approximately symmetric about the equator. Slight minima in T_{CP} are also seen over equatorial Africa and South America, and the minima in T_{CP} are all co-located (in longitude) with the time mean convection (indicated by shading in Figure 5). During NH summer (JJ 1995) the tropical T_{CP} is still relatively cold over the western Pacific, but the cold tropopause extends well northward over the south-Asian monsoon region, near the maximum in convection; for this year the coldest mean T_{CP} were near

20°N (~192 K). The time mean tropopause altitude is relatively low over the tropical western Pacific, where T_{CP} are low, with the height minima slightly west of the temperature minima (see Figure 4). In contrast, the tropopause is relatively high over the cold south-Asian monsoon region (> 17.5 km). There is a seasonal cycle in cold point temperature (~5 K) and altitude (~0.5 km), which is zonally symmetric to first approximation. A slightly larger seasonal cycle in temperature is observed just above the tropopause (~18 km) (as shown below in Figure 14).

The vertical structure of longitudinal temperature anomalies near the equator (10°N-S) during DJF 1996-1997 is shown in Figure 6. Here we have subtracted the zonal mean GPS/MET temperature at each altitude to highlight longitudinal anomalies, and include lines which indicate the cold point tropopause and altitude of minimum lapse rate $\partial\theta/\partial z$ (here θ is potential temperature, $\theta = T(\frac{P}{p_o})^{2/7}$, with $p_0 = 1000$ hPa). The level of minimum $\partial\theta/\partial z$ is associated with the 'top' or level of maximum outflow in tropical convection [in a statistical sense, e.g., *Folkins*, 2000, 2002; *Gettelman and Forster*, 2002], and the region between the minimum $\partial\theta/\partial z$ and cold point tropopause is one definition of the 'tropical tropopause layer' (TTL) [*Gettelman and Forster*, 2002].

Figure 6 shows that the largest tropical temperature anomalies are observed near and below the cold point tropopause, generally within the TTL. The region of strongest time-mean convection near Indonesia (~90-180°E) is associated with warm anomalies over ~10-12 km (centered east of the convection), and coldest anomalies near the (slightly lower) topopause. Note the eastward phase tilt with height of the time average temperature anomalies over ~14-18 km in Figure 6, which is qualitatively similar to the transient response to convection near the equator seen below in Figure 12.

b. Variability in the cold point

A significant amount of sub-seasonal variability is observed in the GPS/MET cold point statistics in Figure 4, and here we examine fluctuations in cold point temperature and height, and study statistical relationships with the temperature profiles and with large-scale convection. Here OLR is used as proxy for tropical convection, and for reference, an OLR threshold below ~ 180-220 K is typically associated with deep convection. We focus on the deep tropics (10°N-S) for DJF 1996-1997, for which there are ~375 GPS/MET observations. The availability of GPS/MET data as a function of longitude and time for this period is shown in Figure 7. This figure also includes shading which indicates location and variability of the most intense convection (OLR < 210 K), plus symbols locating the 5% coldest and 5% warmest T_{CP}.

Figure 8 shows scatter diagrams of the observed variability in cold point temperature and height in the individual GPS/MET soundings during DJF 1996-1997, with data segregated according to deep convective (OLR ≤ 220 K) and non-convective (OLR > 220 K) regions. There is substantial variability in both T_{CP} (values over ~183-195 K) and Z_{CP} (extrema from ~16 to 19 km). However, these scatter diagrams show there is not a strong relationship between temperature and height of the cold point tropopause in individual soundings, either above or away from deep convection. This lack of correlation is somewhat surprising because on seasonal or monthly time scales the coldest T_{CP} are correlated with lowest Z_{CP}, as shown in Figure 5, and also in the radiosonde statistics in *Reid and Gage*, 1996, and *Seidel et al.,* 2001. This distinct behavior between individual soundings and monthly/seasonal statistics is suggestive of additional physical processes for monthly time scales, and one possibility is that radiative effects may be relatively more important for low frequency behavior of the tropopause

[*Thuburn and Craig*, 2000, 2002; *Norton*, 2001; *Hartman et al.,* 2001].

Figure 9a shows the correlation between T_{CP} and the profile of temperature, T(z). These correlations have been calculated from profiles over deep convection (OLR < 220 K), but the results do not depend in detail on the convective environment. Because the cold point is near 17 km, there is strong correlation with T(z) near this altitude (but the correlation is not 1.0, due to the variability of the precise cold point altitude). The cold point temperature is positively correlated with T(z) over a narrow layer, extending approximately 1-2 km above and below the (average) tropopause. Negative correlations are observed 3-5 km below the tropopause, and these are consistent with the vertical phase tilts of waves which contribute to variability in the tropopause region, as shown below.

Similar correlations between Z_{CP} and T(z) are shown in Figure 9b, showing how the height of the tropopause is related to temperatures in the profile. There is virtually no correlation near the (average) tropopause at ~17 km, i.e., no relation between Z_{CP} and T_{CP} (as shown in Figure 8). Positive correlations are found in the layer ~1-3 km below Z_{CP}, i.e., when the cold point is high, T(z) is relatively warm in this layer. Anti-correlations are found for temperatures 1-2 km above Z_{CP}.

The characteristic structure of the temperature profiles with the coldest and warmest cold point tropopauses is shown in Figure 10. Here we show overlaid profiles for the 10 coldest and 10 warmest tropopause samples, together with their respective means and differences. The data in Figure 10 have been sampled over deep convection (OLR ≤ 220 K), but results are similar if no OLR threshold is used. The 'cold tropopause' profiles show a pronounced temperature minimum near ~17 km, whereas the 'warm tropopause' profiles do not exhibit a distinct cold point, but rather the

temperatures are 'flat' over ~15-19 km. The difference between the profiles is near 10 K at 17 km, and oppositely-signed differences are seen below ~14 km (i.e., the 'cold tropopause' profiles are warm below ~ 14 km). This out of phase behavior is consistent with the height-longitude phase tilt of waves revealed using correlations with OLR, as shown below in Figures 12-13. Overall the overlaid profiles in Figure 10 show a large amount of 'wavy' variability in the tropopause region and throughout the stratosphere. This variability is also observed in co-located radiosonde measurements [*Nishida et al.,* 1998], and is probably due to a wide spectrum of tropical waves, such as gravity waves [*Karoly et al*., 1996; *Tsuda et al.,* 2000], Kelvin waves [e.g., *Boehm and Verlinde*, 2000; *Fujiwara et al*., 2001] or other equatorial modes [e.g., *Wheeler and Kiladis*, 1999]. The reality of these waves in the GPS/MET data is further supported by the observed coherence with (independent) OLR measurements, as shown below. The 'snapshot' GPS/MET observations suggest that extrema in these waves amplitude and phase near the tropopause are a primary cause of extreme variability in cold point temperature.

Figure 11 shows a set of similar diagnostics for GPS/MET temperature profiles with the 10 highest and 10 lowest cold point tropopauses. As with temperature, extreme variations of tropopause height appear to be associated with enhanced wave-like variability above ~15 km, and the exact location of wave crests and troughs. Comparison of the mean profiles does not reveal any systematic temperature differences below ~14 km or above ~20 km for the 'high' vs 'low' tropopause cases.

c. Coherence with transient convection

Although the GPS/MET sampling is highly irregular (see Figure 7), it is straightforward to calculate correlations between the individual T(z) profiles and the daily gridded OLR data, taking into account both longitudinal and time lag relationships.

Here we calculate correlations as a function of time and longitude lag between the gridded OLR data and profile GPS/MET data, using the OLR data sampled in latitude closest to the individual GPS/MET observation. These results focus on the time period with most dense sampling and highest quality GPS/MET data during 1-15 February 1997. The overall correlations are not a strong function of time lag (peak near zero days), and we show the longitude-height structure at zero time lag. Auto-correlations for both GPS/MET and OLR data peak strongly near zero time and longitude lags; using a conservative estimate of an e-folding scale of 2 (for time in days, or longitude in 10° bins), correlations above $|r| > 0.26$ are significant at the 95% level for the 190 observations over 10°N-S (Figure 12), and $|r| > 0.31$ are significant for the 135 observations over 10-20°S (Figure 13) [*Lau and Chan*, 1983]. We note that tropical convection rarely penetrates above ~14 km [e.g., *Gettelman et al.,* 2002], so that the patterns revealed in these correlations represent temperatures mostly above the convective region.

Figure 12 shows the height-longitude structure of the correlations between OLR and GPS/MET T(z) for statistics over 10°N-S. Here the contours indicate the spatial patterns of temperature varying coherently (in or out of phase) with convection, and the longitudinal structure shows the temperature response to the east or west of the convective maxima (zero longitude refers to co-located OLR and GPS/MET T(z)). The sign convention is such that positive correlations (shaded in Figure 12) correspond to cold temperatures associated with low OLR (deep convection). The patterns in Figure 12 show significant correlations over the ~12-18 km region, with a clear eastward-tilting phase structure with altitude. The largest correlations (up to 0.5) occur over ~13-16 km, nearly co-located with convection, (i.e., cold anomalies overlying deep convection). Extension

of this pattern to near-tropopause levels (~17 km) occurs 30-60° to the east of the convection, and this is consistent with the cold point extrema highlighted in Figure 7 (east of the Indonesian convection). These cold tropopause anomalies east of convection have also been identified for intraseasonal time scales in the analyses of *Zhou and Holton* [2002]. Relative warm temperature anomalies associated with convection occur in the upper troposphere (~12-16 km) approximately 60-120° to the east of convection. These patterns extend to the tropopause level ~120° east of convection, and this statistical signature is consistent with the extreme warm T_{CP} in Figure 7 near ~240°E, far to the east of Indonesian convection. Also, warm anomalies are observed near the tropopause level in Figure 12, ~60° to the west of convection, consistent with the few extreme warm T_{CP} observed near 60°E in Figure 7. Overall these correlations demonstrate that localized transient tropical convection can influence temperatures in the TTL over longitudes spanning half of the globe. The eastward phase-tilt structure of the patterns in Figure 12 is reminiscent of a Kelvin-wave response to transient convective forcing [*Wheeler et al.,* 2000; *Straub and Kiladis*, 2002], and is also similar to the observed structure of a Madden-Julian Oscillation (MJO) (G. Kiladis, personal communication, 2002). In fact a strong MJO event occurred in the western Pacific during February-March 1997, although the most coherent MJO patterns in OLR were not evident until after the GPS/MET sampling period. It is also interesting to point out that the observed seasonal-mean longitude-height anomaly structure in the equatorial tropopause region (Figure 6) bears a strong resemblance to the transient correlation patterns in Figure 12, in particular for the eastward-tilting cold anomalies above (the time-mean) Indonesian convection, and warm anomalies to the east and west.

Figure 12 also includes a plot of the correlations between OLR and height of the cold point tropopause. Significant positive correlations are observed above and slightly west of convection (note the inverted scale in Figure 12), indicating a low tropopause associated with low OLR (enhanced convection). The relation to the temperature profile correlations in Figure 12 are consistent with Figures 9b and 11, i.e., Z_{cp} variations occur coherently with temperature anomalies over ~14-16 km.

The eastward phase-tilt with height seen in Figure 12 (characteristic of a Kelvin-wave) is peculiar to the temperature-OLR correlations calculated over the equatorial region (10°N-S), and different patterns are observed for other latitudes. For example, Figure 13 shows temperature-OLR correlations calculated for statistics over 10-20°S, showing a distinctive wave-like coherence pattern in the TTL, but with a westward phase tilt with height and zonal scale ~90-120° longitude (zonal wave 3-4). Warm anomalies are observed above convection over ~10-13 km, overlain by cold anomalies spanning ~15-18 km. The occurrence of these temperature patterns over 10-20°S, their westward phase tilt with height in the TTL and zonal wave 3-4 structure, all suggest association with a mixed Rossby-gravity (MRG) mode [e.g., *Holton*, 1972; *Wheeler et al.,* 2000]. However, the fact that the correlation patterns in Figure 13 are significant only for temperatures to the west of convection is unexpected for MRG waves (which have an eastward group velocity), and these patterns are different from the more symmetric patterns derived from long data records [*Wheeler et al*., 2000]. This behavior is puzzling and is unexplained at present. In any case, the important points are that (1) the GPS/MET temperatures show strong correlation with OLR in the TTL, and (2) the wave-like patterns demonstrate an influence of convection which is highly non-local in longitude.

5. Annual Cycle and the QBO

Further aspects of tropical temperature variability are revealed by analysis of the entire GPS/MET data set covering 1995-1997. Figure 14 shows all of the measurements near the equator (± 4° latitude) at 18 km for the GPS/MET record, together with the annual cycle derived by harmonic regression analysis. This shows the well-known annual cycle in temperature near and above the tropical tropopause, with minima during NH winter [e.g., *Yulaeva et al.,* 1994; *Reid and Gage*, 1996]. Figure 15 shows a meridional cross section of the amplitude of the annual cycle in temperature derived from the GPS/MET data, showing that the large annual cycle in the tropics occurs over a relatively narrow vertical layer near and above the tropopause (~16-22 km). The maximum amplitude of the tropical annual cycle in GPS/MET data is ~8 K (near 18 km), somewhat larger than that derived from radiosondes [*Reed and Vlcek*, 1969] or meteorological analyses [*Rosenlof*, 1995]. The fact that the large annual cycle in tropical temperature occurs only over ~16-22 km is explained quantitatively by the long radiative damping time scales in this region; the temperature response to the annual cycle in the upward Brewer-Dobson circulation is magnified in this region by radiative time scales of order 100 days [*Randel et al.,* 2002].

Interannual anomalies in the GPS/MET data are studied by calculating monthly means, subtracting the annual cycle at each latitude and height, and interpolating across months with no data. Figure 16 shows an altitude-time section of temperature anomalies over the equator (± 4° latitude), showing downward propagating patterns over the depth of the stratosphere with an approximate 2-year periodicity. These anomalies are associated with the stratospheric QBO [*Baldwin et al.,* 2001]. The space-time patterns in Figure 16 are very similar to QBO patterns for this time period in UKMO stratospheric analyses [*Randel et al.,* 1999], but the magnitudes are somewhat larger in the higher

vertical resolution GPS/MET data (as can be seen in Figure 3). Figure 17 shows time series of the GPS/MET zonal mean temperature anomalies at several levels, compared with a longer record of radiosonde data from one location (Singapore, at 1°N). The longer Singapore record clearly shows the dominance of the QBO in the tropical stratosphere, and there is excellent agreement with the GPS/MET observations during the overlap period April 1995-February 1997. Further confirmation of the QBO signature is seen in the latitudinal structure of the GPS/MET temperature anomalies at 24 km shown in Figure 18. Here the tropical temperature anomalies are found to be clearly centered over the equator, with out-of-phase temperature patterns observed in subtropics of each hemisphere [consistent with the QBO meridional circulation, e.g., *Baldwin et al.,* 2001].

6. Summary and Discussion

GPS/MET was designed as a demonstration system to explore the utility of satellite radio occultation measurements, and the system was operational for almost two years. The GPS/MET measurements provide high vertical resolution temperature profile data, and these agree extremely well with co-located radiosonde measurements in the tropics over ~10-30 km. The spatial sampling of GPS/MET is high for several time periods and this study has focused on the structure and variability of temperatures near the tropical tropopause, and their relationship to convection, in addition to seasonal and interannual variability.

The spatial structure and seasonality of the cold point tropical tropopause derived from GPS/MET data agree with previous analyses. There is little correlation between temperature and height of the cold point in individual measurements, in contrast to the negative correlation observed in seasonal or monthly mean data [e.g., *Seidel et al.,* 2001]. This suggests that different or additional mechanisms are important for maintaining the

cold point on monthly time scales, such as radiative forcing. The majority of tropopause temperature or height variability in the 'snapshot' GPS/MET observations appears to be related to wave-like variability (i.e., the exact location of crests or troughs). This variability is ubiquitous in the GPS/MET tropical temperature profiles above ~15 km, and the reality of these waves is supported by evidence in co-located radiosondes [*Nishida et al.,* 2000], and by the observed coherence with independent OLR data shown here. *Tsuda et al.* [2000] examined the wave-like variations in GPS/MET temperature profile data in some detail, finding strong variance for vertical wavelengths of ~2-10 km, maximum amplitudes in the tropics (in particular near convection), and extratropical seasonality consistent with gravity waves. Alexander et al. [2002] show that the latitudinal structure of wave variance in GPS/MET data (in particular the tropical maximum) is consistent with theoretical expectations for inertia gravity waves. Our results suggest that such wave variability, due to inertia-gravity waves, or other tropical oscillations such as Kelvin waves [*Boehm and Verlinde*, 2000; *Fujiwara et al.,* 2001; *Straub and Kiladis,* 2002], is a key component of tropical tropopause behavior.

Correlations between the GPS/MET temperatures and daily gridded OLR data delineate the temperature response to transient deep convection in the tropical tropopause layer. For the time period analyzed here the temperature correlations near the equator show a local and remote response to localized convective maxima which cover over 180° in longitude (Figure 12), and have a characteristic eastward phase tilt with height in the TTL. A cool region is observed co-located with convection over the ~13-16 km layer; however, maximum cold anomalies at tropopause level (~17 km) are observed ~30-60° to the east, while warm anomalies are observed ~ 120° to the east and ~60-90° to the west of the convective center. Thus the relatively warm tropopause temperatures over the

equatorial eastern Pacific and Indian oceans seen in Figure 7 are correlated with transient convection over Indonesia. Away from the equator the specific correlation patterns are very different (Figure 13), but still show wave-like coherence extending over a hemisphere. Note that there are cold anomalies in the TTL above convection in both the equatorial (Figure 12) and off-equatorial (Figure 13) statistics. These could be a signature of convective overshooting [as in the model of *Sherwood and Dessler*, 2001], or the wave-like temperature patterns in the TTL could be a characteristic wave response to convective heating in the lower-middle troposphere [e.g., *Holton*, 1972; *Garcia and Salby*, 1987; *Wheeler et al.,* 2000]; one possibility is that the two effects may reinforce each other. An interesting additional result is that the time mean thermal structure of the TTL over the equator (Figure 6) exhibits longitude-height patterns which are related to the time mean convection in a similar fashion as the transient equatorial statistics (Figure 12). This similarity to a Kelvin wave response may help explain the approximate symmetry of the cold Indonesian tropopause region centered over the equator in DJF (Figure 5), when convection is south of the equator.

The almost two years of GPS/MET coverage also allows analyses of seasonal and interannual temperature variations over ~10-40 km. The seasonal cycle of temperature is large in a relatively narrow vertical layer near and above the tropical tropopause, over ~16-22 km, and this is quantitatively explained by the seasonal cycle in the extratropically-forced Brewer-Dobson upwelling coupled with the long radiative time scales in the tropical lower stratosphere [Randel et al., 2002]. The GPS/MET data also show clear evidence of the stratospheric QBO in temperature during 1995-1997, with downward propagating temperature anomalies centered over the equator, with amplitudes of ~ ± 3-5 K. These QBO patterns are evident over altitudes ~40-16 km (Figure 16), and

reach the tropopause level with amplitudes ~ ± 0.5 K.

Overall the geophysical variability evident in the tropical GPS/MET temperature data are consistent with previous observations, and the high vertical resolution and dense spatial sampling of GPS radio occultation provides improved level of detailed understanding. Ongoing and future GPS missions [e.g., CHAMP, *Wickert et al*., 2001; SAC-C, *Hajj et al.,* 2002; COSMIC, *Anthes et al.,* 2000] will offer the opportunity for enhanced space-time sampling and long-term coverage of the tropical tropopause region. In particular, COSMIC plans to have six orbiting GPS receivers, and will provide daily sampling similar to the seasonal coverage obtained by GPS/MET (Figure 1).

Acknowledgments

We thank Rick Anthes, Andy Dessler, Rolando Garcia, Jim Holton, George Kiladis, Jean-Francois Lamarque, Chris Rocken and Kathy Straub for discussions during the course of this work, and comments on the paper. Marilena Stone expertly prepared the manuscript. Waleska Rivera-Rios was supported at NCAR by the Significant Opportunities in Atmospheric Research and Science (SOARS) program during 1999-2000. This work is partially supported under NASA ACMAP grant W-18181. The National Center for Atmospheric Research is operated by the University Corporation for Atmospheric Research under the sponsorship of the National Science Foundation.

References

1. Alexander, M. J., T. Tsuda, and R. A. Vincent, 2002: Latitude variations observed in gravity waves with short vertical wavelengths. *J. Atmos. Sci.,* **59**, 1394-1404.
2. Anthes, R., C. Rocken, and Y.-H. Kuo, 2000: Applications of COSMIC to meteorology and climate. *Terrestial, Atmospheric and Oceanic Sciences*, **11**, 31-50.
3. Baldwin, M. P., and co-authors, 2001: The quasi-biennial oscillation. *Rev. Geophys.*, **39**, 179-229.
4. Boehm, M. T., and J. Verlinde, 2000: Stratospheric influence on upper tropospheric tropical cirrus. *Geophys. Res. Lett.,* **27**, 3209-3212.
5. Folkins, I., S. J. Oltmans, and A. M. Thompson, 2000: Tropical convective outflow and near-surface equivalent potential temperature. *Geophys. Res. Lett.,* **27**, 2549-2552.
6. Folkins, I., 2002: Origin of lapse rate changes in the upper tropical troposphere. *J. Atmos. Sci.,* in press.
7. Fujiwara, M., F. Hasebe, M. Shiotani, N. Nishi, H. Vomel, and S. J. Oltmans, 2001: Water vapor control at the tropopause by equatorial Kelvin waves observed over the Galapagos. *Geophys. Res. Lett*., **28**, 3143-3146.
8. Garcia, R. R., and M. L. Salby, 1987: Transient response to localized episodic heating in the tropics. Part II: Far-field behavior. *J. Atmos. Sci.,* **44**, 499-530.
9. Gettelman, A., M. Salby, and F. Sassi, 2002: The distribution and influence of convection in the tropical tropopause region. *J. Geophys. Res.,* in press.

10. Gettelman, A., and P. M. de F. Forster, 2002: Definition and climatology of the tropical tropopause layer. *J. Meteorol. Soc. Japan*, in press.

11. Hajj, G. A., M. dela Torre Juarez, B. A. Iijima, E. R. Kursinski, A. J. Mannucci, and T. P. Yunck, 2002: GPS Radio Occultations coming of age: Spacecraft launches add two new instruments for climate monitoring. *EOS Transactions,* Vol. **83**, No. 4, p. 37, 22 Jan. 2002.

12. Hartman, D. L., J. R. Holton, and Q. Fu, 2001: The heat balance of the tropical tropopause, cirrus and stratospheric dehydration. *Geophys. Res. Lett.,* **28**, 1969-1972.

13. Highwood, E. J., and B. J. Hoskins, 1998: The tropical tropopause. *Q.J.R. Meteorol. Soc.*, **124**, 1579-1604.

14. Hoinka, K. P., 1999: Temperature, humidity and wind at the global tropopause. *Mon. Wea. Rev.,* **127**, 2248-2265.

15. Holton, J. R., 1972: Waves in the equatorial stratosphere generated by tropospheric heat sources. *J. Atmos. Sci.,* **29**, 368-375.

16. Jensen, E. J., O. B. Toon, H. B. Selkirk, J. D. Spinhirne, and M. R. Schoeberl, 1996: On the formation and persistence of subvisible cirrus clouds near the tropical tropopause. *J. Geophys. Res.,* **101**, 21,361-21,375.

17. Kalnay, E., and co-authors, 1996: The NCEP-NCAR 40-year reanalysis project. B*ull. Am. Meteorol. Soc.,* 77, 437-471.

18. Karoly, D. J., G. L. Roff, and M. J. Reeder, 1996: Gravity wave activity associated with tropical convection detected in TOGA COARE. *Geophys. Res. Lett.*, **23**, 261-264.

19. Kiladis, G. N., K. H. Straub, G. C. Reid, and K. S. Gage, 2000: Aspects of interannual and intraseasonal variability of the tropopause and lower stratosphere. *Q.J.R. Meteorol. Soc.,* **126**, 1-16.

20. Kursinski, E. R., et al., 1996: Initial results of radio occultation observations of Earth's atmosphere using the Global Positioning System. *Science*, **271**, 1107-1110.

21. Kursinski, E. R., G. A. Hajj, J. T. Schofield, R. P. Linfield, and K. R. Hardy, 1997: Observing Earth's atmosphere with radio occultation measurements using the Global Positioning System. *J. Geophys. Res.,* **102**, 23,429-23,465.

22. Lau, K.-M., and P. H. Chan, 1983: Short-term climate variability and atmospheric teleconnections from satellite-observed outgoing longwave radiation. Part II: Lagged correlations. *J. Atmos. Sci.,* **40**, 2751-2767.

23. Massie, S. T., A. Gettelman, W. Randel, and D. Baumgardner, 2002: The distribution of tropical cirrus in relation to convection. *J. Geophys. Res*., accepted.

24. Nishida, M., A. Shimizu, T. Tsuda, C. Rocken, and R. H. Ware, 2000: Seasonal and longitudinal variations in the tropical tropopause observed with the GPS occultation technique (GPS/MET). *J. Meteorol. Soc. Japan*, **78**, 691-700.

25. Norton, W. A., 2001: Longwave heating of the tropical lower stratosphere. *Geophys. Res. Lett.,* **28**, 3653-3656.

26. Pawson, S., and M. Fiorino, 1998: A comparison of reanalyses in the tropical stratosphere. Part I: Thermal structure and the annual cycle. *Clim. Dyn.,* **14**, 631-644.

27. Randel, W. J., F. Wu, R. Swinbank, J. Nash, and A. O'Neill, 1999: Global QBO circulation derived from UKMO stratospheric analyses. *J. Atmos. Sci.,* **56**, 457-474.

28. Randel, W. J., F. Wu, and D. Gaffen, 2000: Interannual variability of the tropical tropopause derived from radiosonde data and NCEP reanalyses. *J. Geophys. Res.,* **105**, 15,509-15,523.

29. Randel, W. J., R. R. Garcia, and F. Wu, 2002: Time dependent upwelling in the tropical lower stratosphere estimated from the zonal mean momentum budget. *J. Atmos. Sci.*, **59**, 2141-2152.

30. Reed, R. J., and C. L. Vlcek, 1969: The annual temperature variation in the lower tropical stratosphere. *J. Atmos. Sci.,* **26**, 163-167.

31. Reid, G., and K. Gage, 1996: The tropical tropopause over the western Pacific: Wave driving, convection and the annual cycle. *J. Geophys. Res.,* **101**, 21,233-21,241.

32. Rocken, C., and co-authors, 1997: Analysis and validation of GPS/MET data in the neutral atmosphere. *J. Geophys. Res.,* **102**, 29,849-29,866.

33. Rosenlof, K. H., 1995: Seasonal cycle of the residual mean meridional circulation in the stratosphere. *J. Geophys. Res.,* **100**, 5173-5192.

34. Seidel, D. J., R. J. Ross, J. K. Angell, and G. C. Reid, 2001: Climatological characteristics of the tropical tropopause as revealed by radiosondes. *J. Geophys. Res.*, **106**, 7857-7878.

35. Sherwood, S., and A. Dessler, 2001: A model for transport across the tropical tropopause. *J. Atmos. Sci.,* **58**, 765-779.

36. SPARC Assessment of Upper Tropospheric and Stratospheric Water Vapor. SPARC Report No. 2, WCRP Report No. 113, WMO/TD-No. 1043, December 2000.

37. Straub, K. H., and G. Kiladis, 2002: Observations of a convectively coupled Kelvin wave in the eastern Pacific ITCZ. *J. Atmos. Sci.,* **59**, 30-53.

38. Swinbank, R., and A. O'Neill, 1994: A stratosphere-troposphere data assimilation system. *Mon. Wea. Rev.,* **122**, 686-702.

39. Thuburn, J., and G. C. Craig, 2000: Stratospheric influence on tropopause height: the radiative constraint. *J. Atmos. Sci.,* **57**, 17-28.

40. Thuburn, J., and G. C. Craig, 2002: On the temperature structure of the tropical substratosphere. *J. Geophys. Res*., **107**, 10.1029/2001JD000448.

41. Tsuda, T., and co-authors, 1994: Variations of gravity wave characteristics with height, season and latitude revealed by comparative observations. *J. Atmos. Sol. Terr. Phys*., **56**, 555-568.

42. Tsuda, T., M. Nishida, C. Rocken, and R. H. Ware, 2000: A global morphology of gravity wave activity in the stratosphere revealed by the GPS Occultation Data (GPS/MET). *J. Geophys. Res.,* **105**, 7257-7273.

43. Wheeler, M., and G. N. Kiladis, 1999: Convectively coupled equatorial waves: Analysis of clouds and temperature in the wavenumber-frequency domain. *J. Atmos. Sci*., **56**, 374-399.

44. Wheeler, M., G. N. Kiladis, and P. J. Webster, 2000: Large-scale dynamical fields associated with convectively coupled equatorial waves. *J. Atmos. Sci*., **57**, 613-640.

45. Wickert, J., and co-authors, 2001: Atmosphere sounding by GPS radio occultation: First results from CHAMP. *Geophys. Res. Lett.,* **28**, 3263-3266.

46. Yulaeva, E., J. R. Holton, and J. M. Wallace, 1994: On the cause of the annual cycle in the lower topical stratospheric temperature. *J. Atmos. Sci.,* **51**, 169-174.

47. Zhou, X., and J. R. Holton, 2002: Intraseasonal variations of tropical cold-point tropopause temperatures. *J. Climate*, **15**, 1460-1473.

Figure 1. Spatial sampling of GPS/MET temperature data during (a) June-July 1995 and (b) December-February 1996-1997.

Figure 2. Left panel shows vertical profiles of (GPS/MET-radiosonde) mean and rms temperature difference statistics, for tropical measurements over 20°N-20°S. The statistics are separated according to GPS/MET measurements made during so-called prime periods (June-July 1995 and February 1997) and off-prime periods (all other months during 1995-1997). The right panel shows the corresponding number of comparisons at each altitude.

Figure 3. Vertical profile of tropical mean temperature over 10°N-10°S during January 1-15, 1997, derived from GPS/MET and from a number of meteorological analyses (as noted).

Figure 4. (a) Scatter diagram of cold point tropopause temperature (K) versus longitude during DJF 1996-1997, showing all the observations over 10°N-10°S. The central line shows the average. (b) Similar statistics for the cold point tropopause altitude.

Figure 5. Time average spatial structure of the cold point tropopause temperature (left) and altitude (right), for statistics during June-July 1995 (top) and December-February 1996-1997 (bottom). Shading in the left panels denotes regions of strongest convection (OLR < 210 K). The contour interval for height is 0.2 km, and values above 17.4 km are shaded.

Figure 6. Height-longitude section of temperature anomalies (departures from the zonal mean) over 10°N-10°S, during DJF 1996-1997. Contour interval is 0.5 K, with zero contours omitted. The solid line near 17 km is the cold point tropopause,

and the dashed line near 13 km denotes the altitude of the minimum lapse rate. The curve at the bottom shows the corresponding time mean OLR structure over 10°N-S, indicating regions of maximum convection.

Figure 7. Longitude-time section showing the location of all of the GPS/MET temperature measurements over 10°N-10°S during DJF 1996-1997. The open circles denote the 5% coldest T_{CP}, and the filled circles denote the 5% warmest T_{CP}. Shading indicates regions of deepest convection (OLR < 210 K).

Figure 8. Scatter diagrams of cold point tropopause height versus temperature, separated for observations over deep convection (OLR ≤ 220) and away from convection (OLR > 220). The right and top axes of each panel show the corresponding histogram distributions.

Figure 9. (a) Vertical profile of correlation between cold point temperature and temperature at each altitude, derived from temperature profiles over deep convection (OLR < 220 K). (b) Corresponding correlation between cold point height and temperature at each altitude. Error bars denote the 2 x sigma uncertainties for the correlations.

Figure 10. Overlaid altitude profiles of temperature for the 10 coldest (top) and 10 warmest (middle) cold point tropopauses over 10°N-10°S during December-February 1996-1997. Bottom panel shows the corresponding means, and their difference. The hatched area near the zero difference line indicates the 95% statistical significance level for the mean differences, derived from resampling the entire population of tropical soundings.

Figure 11. As in Figure 10, but for the 10 highest (top) and 10 lowest (middle) cold point tropopauses, together with their means and differences (bottom).

Figure 12. Correlation between near-equatorial GPS/MET temperatures profiles and contemporaneous OLR measurements, as a function of longitude lag. Calculations are based on all the GPS/MET temperature profiles over 10°N-10°S during 1-15 February 1997. Contours are ± 0.20, 0.30, 0.40, … .The line on the top indicates correlations between OLR and the cold point height.

Figure 13. As in Figure 12, but for correlation statistics calculated over 10-20°S. Contours are ± 0.20, 0.30, 0.40, …

Figure 14. Time series of GPS/MET temperatures at 18 km over 4°N-S, together with the annual cycle derived by harmonic analysis.

Figure 15. Amplitude of the annual cycle in temperature (K), derived from GPS/MET data during April 1995-February 1997. The heavy line near 17 km denotes the cold point tropopause.

Figure 16. Height-time series of deseasonalized temperature anomalies over the equator (4°N-4°S), derived from GPS/MET data. Contours are ± 0.5, 1.5, 2.5, …K. Heavy line denotes the cold point tropopause.

Figure 17. Time series of equatorial temperature anomalies at several pressure levels, comparing Singapore radiosondes (1993-1997) with GPS/MET zonal means for April 1995-February 1997. Both data sets were normalized to zero time average for the GPS/MET time period, and the monthly Singapore data were smoothed with a 1-2-1 running mean.

Figure 18. Latitude-time diagram of interannual temperature anomalies at 24 km, derived from GPS/MET data. Contours are ± 0.5, 1.5, 2.5, … K.

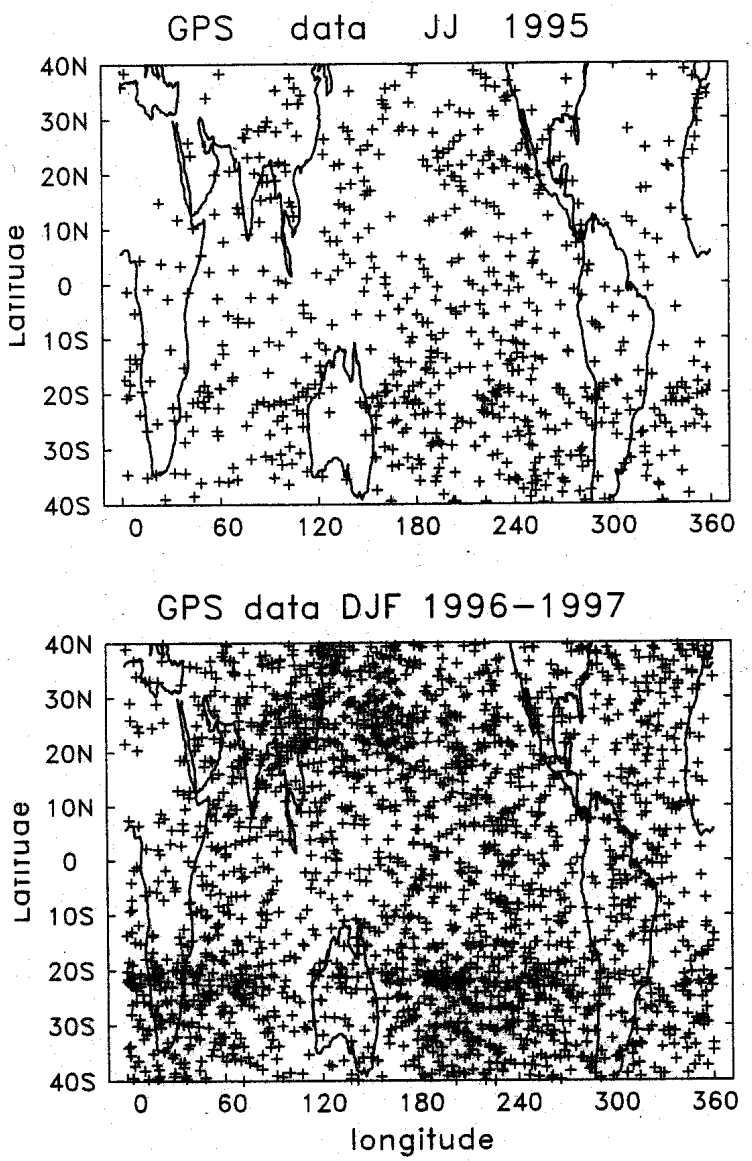

Figure 1. Spatial sampling of GPS/MET temperature data during (a) June-July 1995 and (b) December-February 1996-1997.

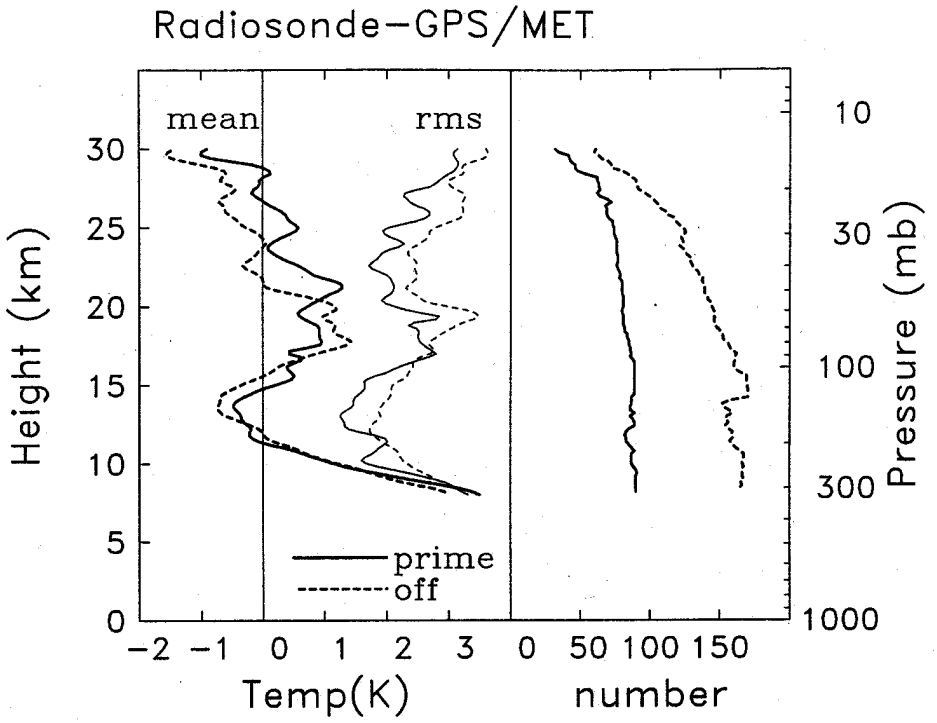

Figure 2. Left panel shows vertical profiles of (GPS/MET-radiosonde) mean and rms temperature difference statistics, for tropical measurements over 20°N-20°S. The statistics are separated according to GPS/MET measurements made during so-called prime periods (June-July 1995 and February 1997) and off-prime periods (all other months during 1995-1997). The right panel shows the **corresponding number of comparisons at each altitude.**

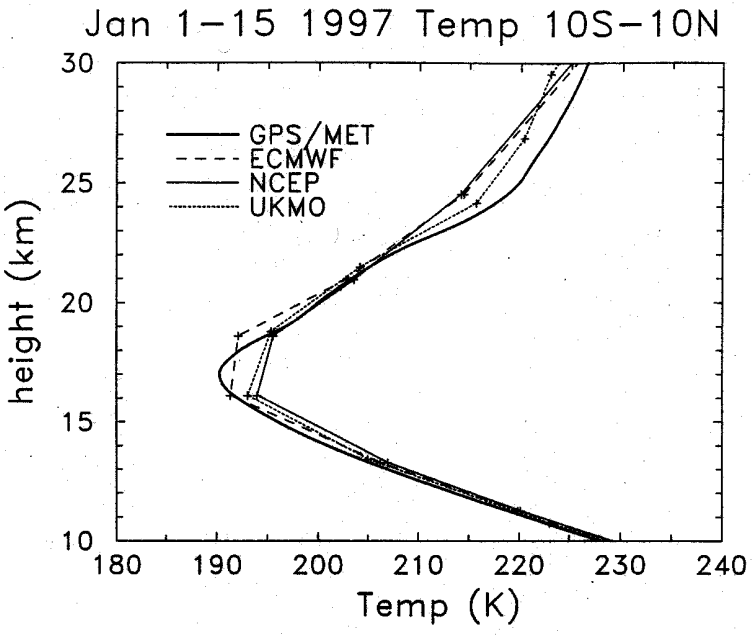

Figure 3. Vertical profile of tropical mean temperature over 10°N-10°S during January 1-15, 1997, derived from GPS/MET and from a number of meteorological analyses (as noted).

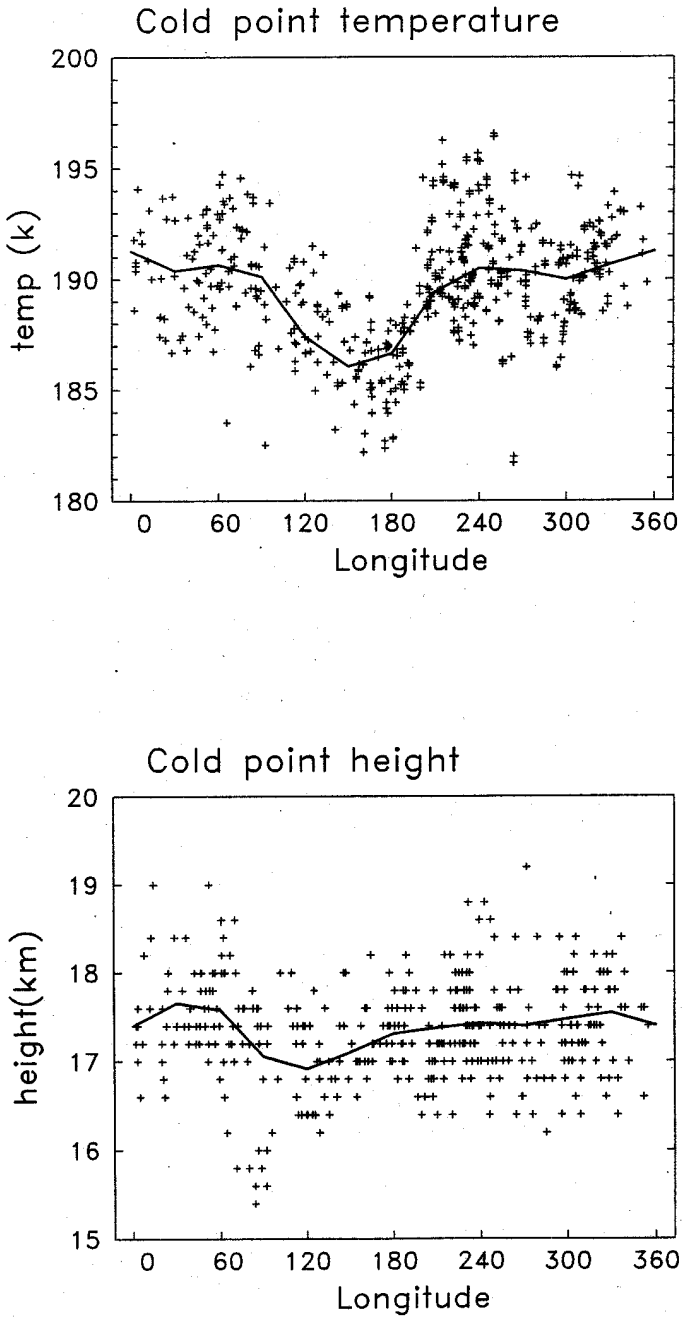

Figure 4. (a) Scatter diagram of cold point tropopause temperature (K) versus longitude during DJF 1996-1997, showing all the observations over 10°N-10°S. The central line shows the average. (b) Similar statistics for the cold point **tropopause altitude.**

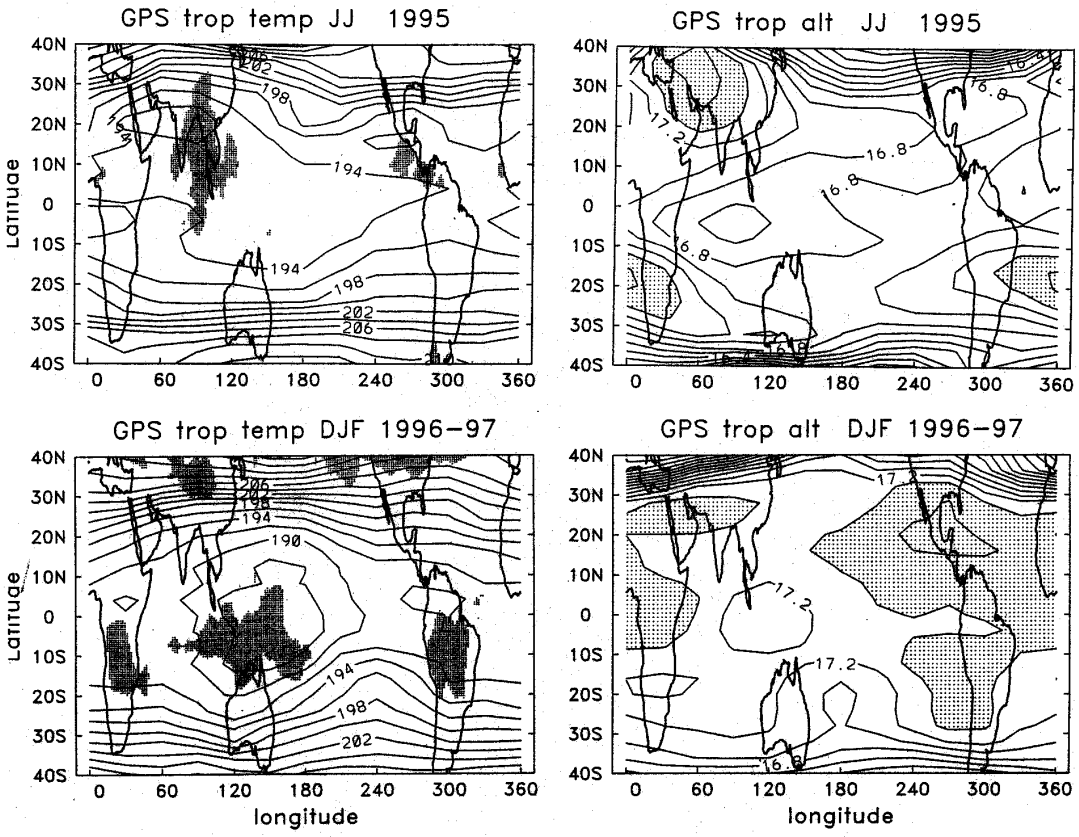

Figure 5. Time average spatial structure of the cold point tropopause temperature (left) and altitude (right), for statistics during June-July 1995 (top) and December-February 1996-1997 (bottom). Shading in the left panels denotes regions of strongest convection (OLR < 210 K). The contour interval for height is 0.2 km, and values above 17.4 km are shaded.

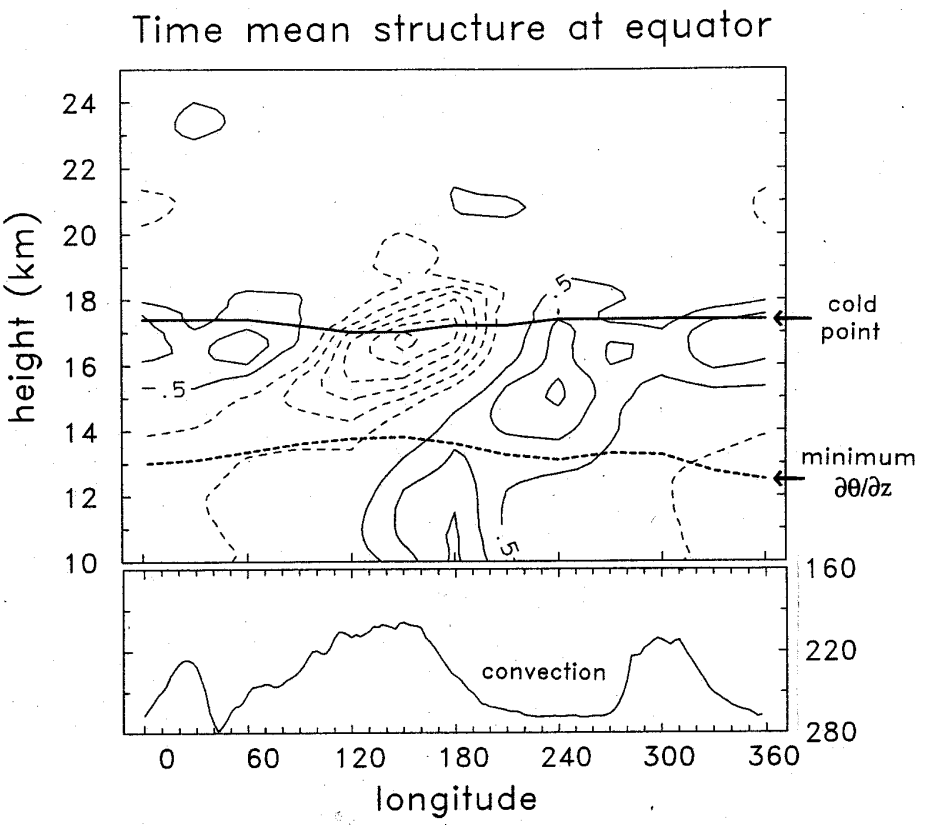

Figure 6. Height-longitude section of temperature anomalies (departures from the zonal mean) over 10°N-10°S, during DJF 1996-1997. Contour interval is 0.5 K, with zero contours omitted. The solid line near 17 km is the cold point tropopause, and the dashed line near 13 km denotes the altitude of the minimum lapse rate. The curve at the bottom shows the corresponding time mean OLR structure over 10°N-S, indicating regions of maximum convection.

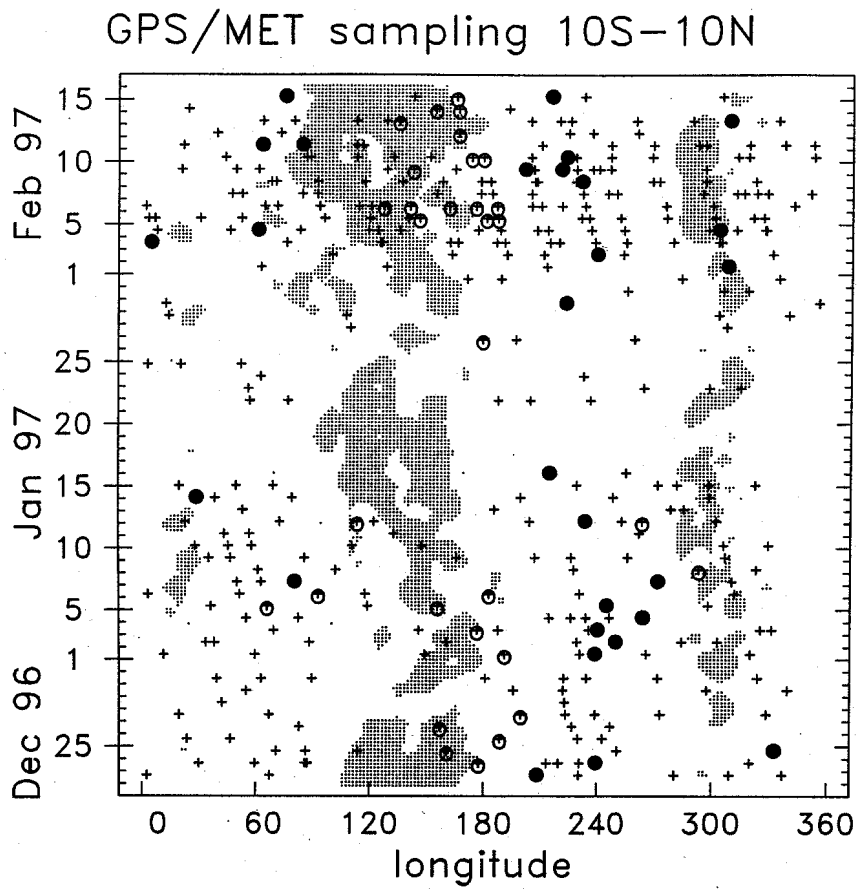

Figure 7. Longitude-time section showing the location of all of the GPS/MET temperature measurements over 10°N-10°S during DJF 1996-1997. The open circles denote the 5% coldest T_{CP}, and the filled circles denote the 5% warmest T_{CP}. Shading indicates regions of deepest convection (OLR < 210 K).

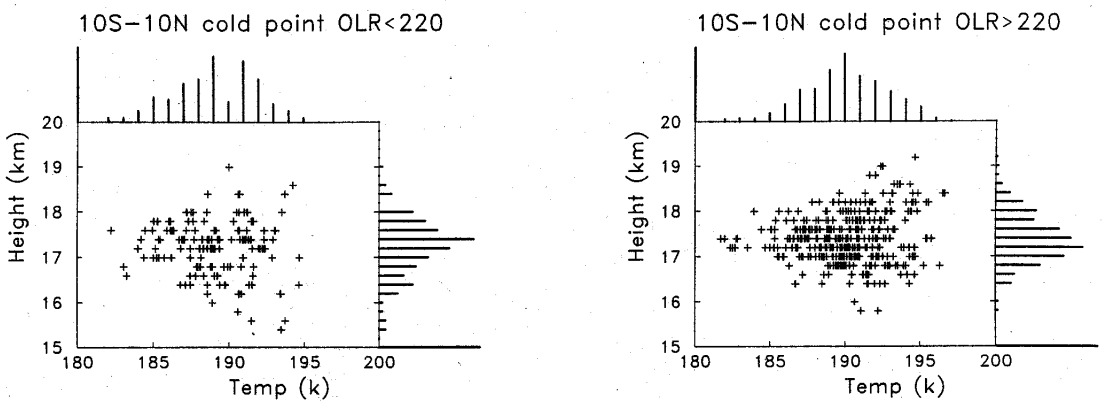

Figure 8. Scatter diagrams of cold point tropopause height versus temperature, separated for observations over deep convection (OLR ≤ 220) and away from convection (OLR > 220). The right and top axes of each panel show the corresponding **histogram distributions.**

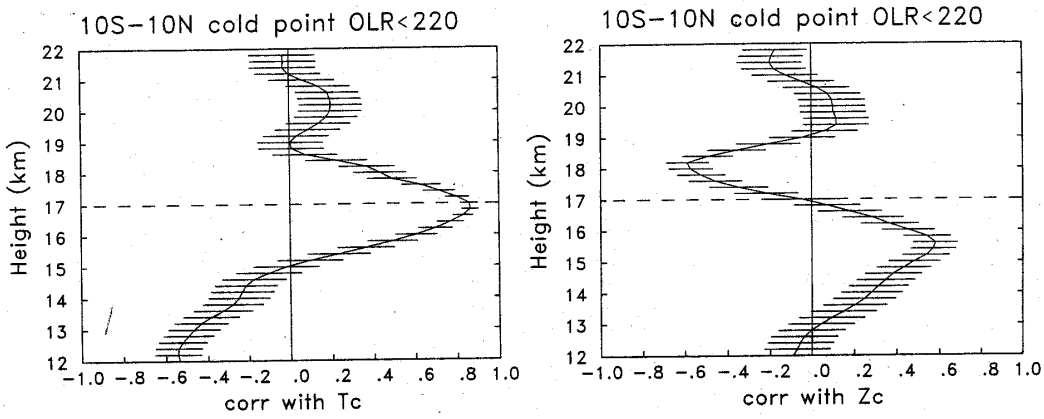

Figure 9. (a) Vertical profile of correlation between cold point temperature and temperature at each altitude, derived from temperature profiles over deep convection (OLR < 220 K). (b) Corresponding correlation between cold point height and temperature at each altitude. Error bars denote the 2 x sigma **uncertainties for the correlations.**

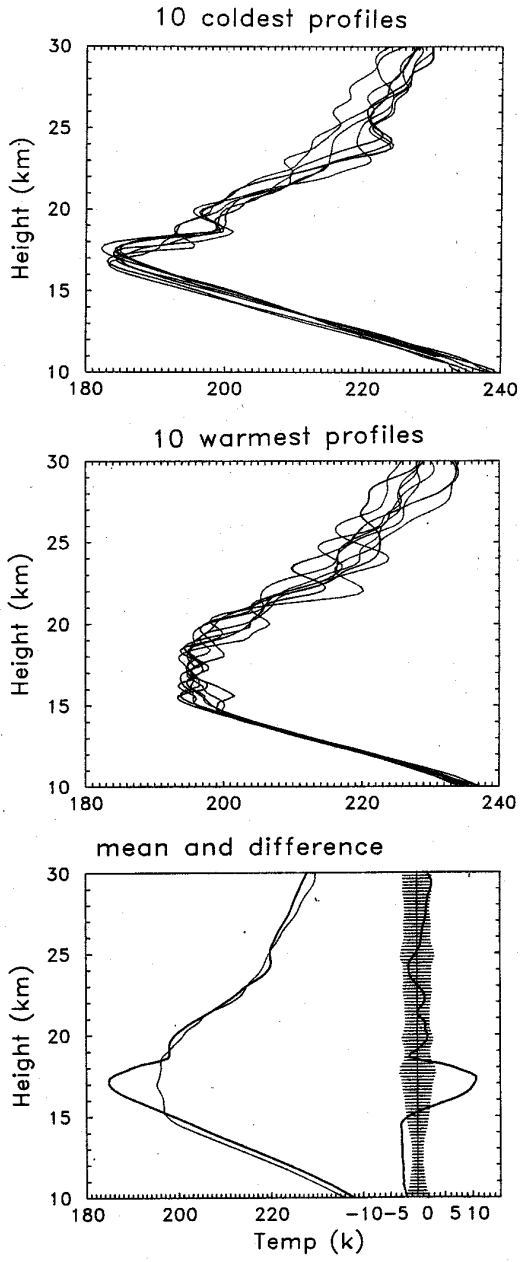

Figure 10. Overlaid altitude profiles of temperature for the 10 coldest (top) and 10 warmest (middle) cold point tropopauses over 10°N-10°S during December-February 1996-1997. Bottom panel shows the corresponding means, and their difference. The hatched area near the zero difference line indicates the 95% statistical significance level for the mean differences, derived from resampling **the entire population of tropical soundings.**

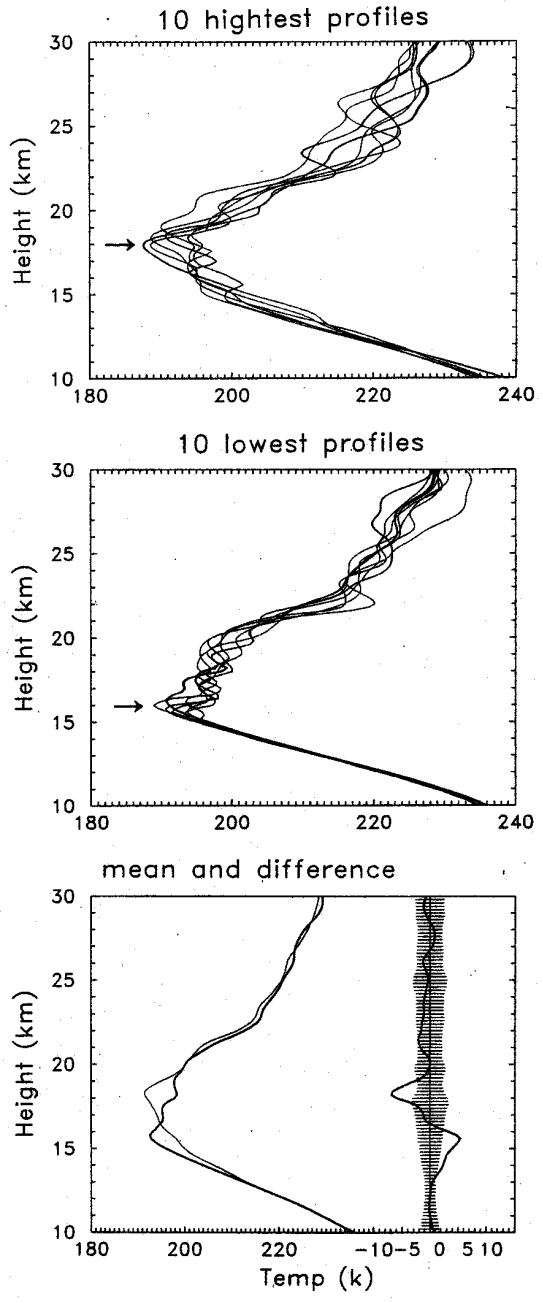

Figure 11. As in Figure 10, but for the 10 highest (top) and 10 lowest (middle) cold point tropopauses, together with their means and differences (bottom).

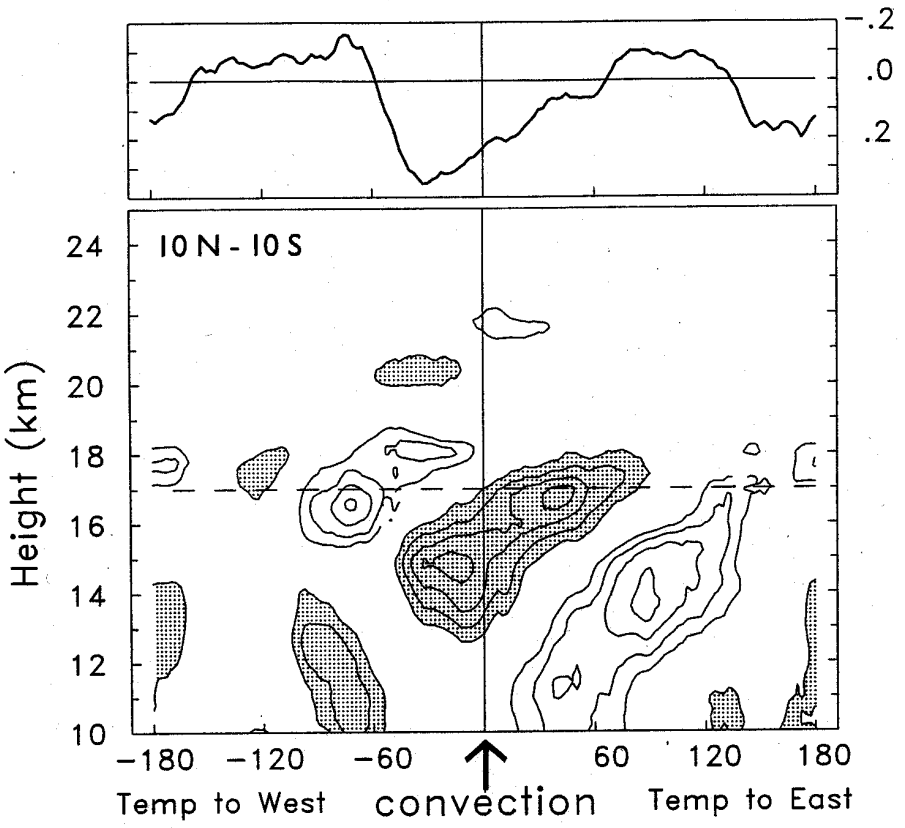

Figure 12. Correlation between near-equatorial GPS/MET temperatures profiles and contemporaneous OLR measurements, as a function of longitude lag. Calculations are based on all the GPS/MET temperature profiles over 10°N-10°S during 1-15 February 1997. Contours are ± 0.20, 0.30, 0.40, … .The line on the top indicates correlations between OLR and the cold point height.

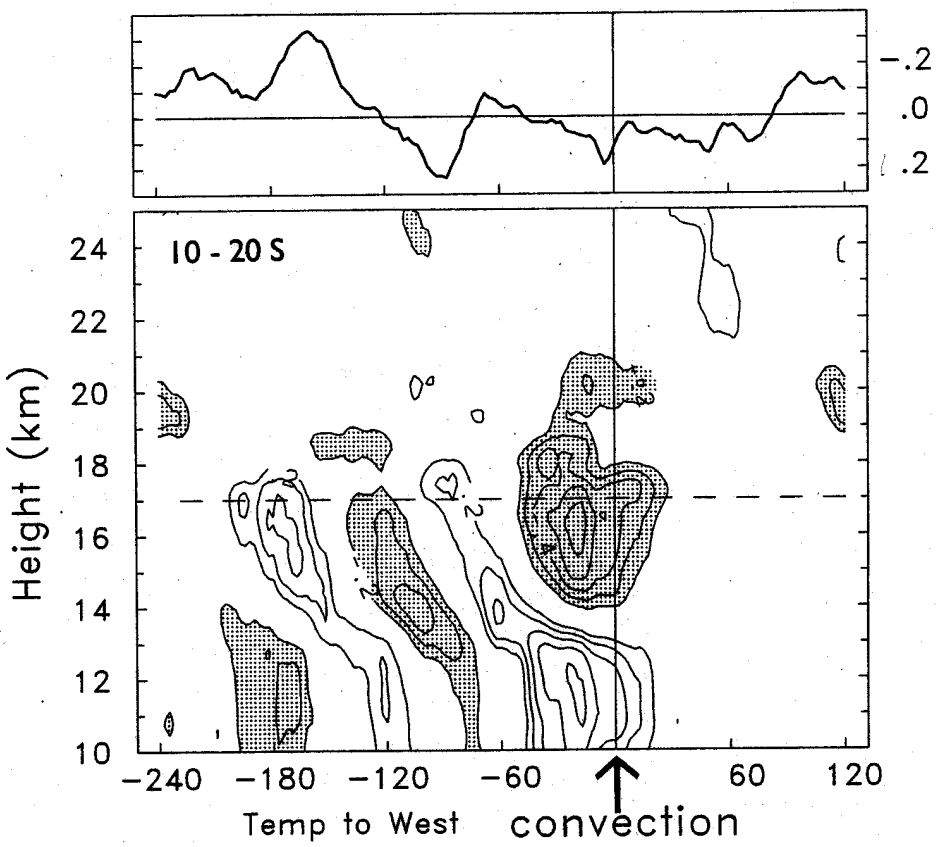

Figure 13. As in Figure 12, but for correlation statistics calculated over 10-20°S.

Contours are ± 0.20, 0.30, 0.40, ...

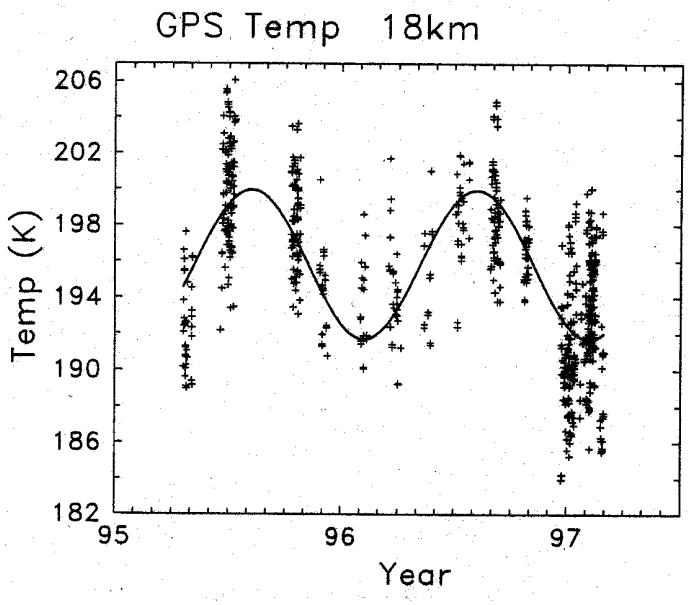

Figure 14. Time series of GPS/MET temperatures at 18 km over 4°N-S, together with the annual cycle derived by harmonic analysis.

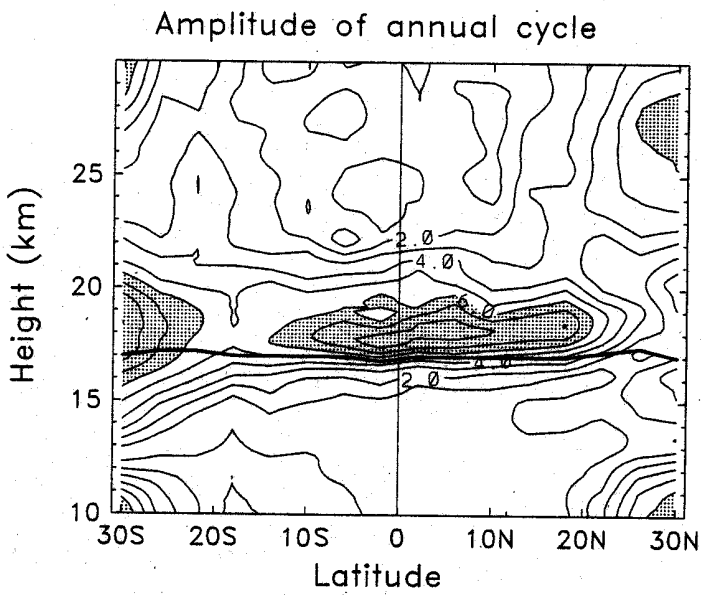

Figure 15. Amplitude of the annual cycle in temperature (K), derived from GPS/MET data during April 1995-February 1997. The heavy line near 17 km denotes the cold point tropopause.

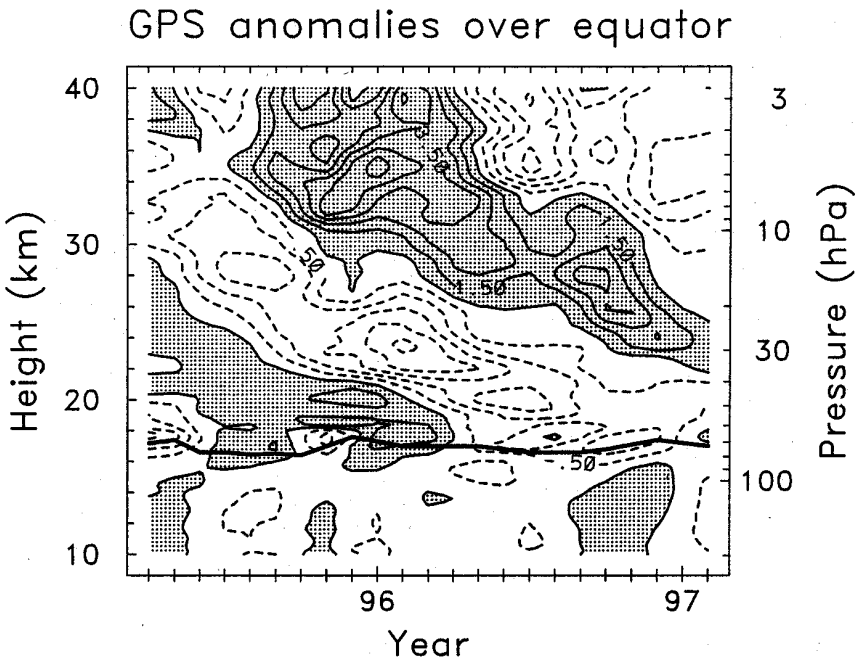

Figure 16. Height-time series of deseasonalized temperature anomalies over the equator (4°N-4°S), derived from GPS/MET data. Contours are ± 0.5, 1.5, 2.5, ...K. Heavy line denotes the cold point tropopause.

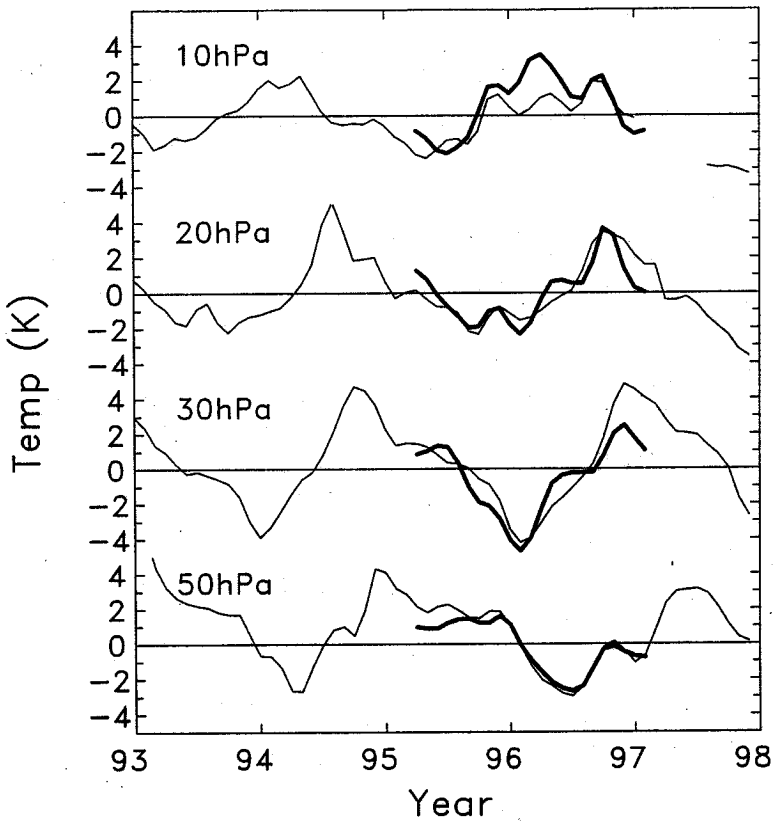

Figure 17. Time series of equatorial temperature anomalies at several pressure levels, comparing Singapore radiosondes (1993-1997) with GPS/MET zonal means for April 1995-February 1997. Both data sets were normalized to zero time average for the GPS/MET time period, and the monthly Singapore data were smoothed with a 1-2-1 running mean.

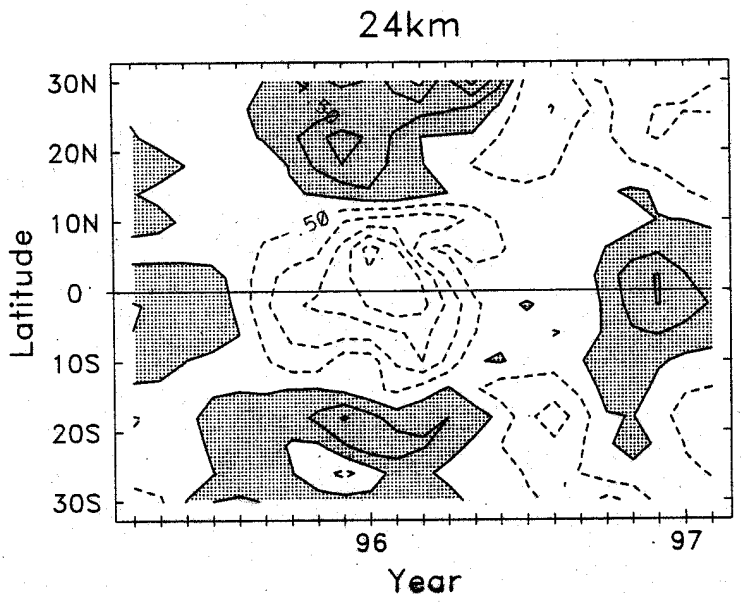

Figure 18. Latitude-time diagram of interannual temperature anomalies at 24 km, derived from GPS/MET data. Contours are ± 0.5, 1.5, 2.5, ... K.